# Identification of Novel and Differentially Expressed MicroRNAs in Goat Enzootic Nasal Adenocarcinoma

Wang Bin[1], Ye Ni[1#], Cao San-jie[1], Wen Xin-tian[1], Huang Yong[1], Yan Qi-gui[1&*]

Wang Bin binwang2@163.com Sichuan Agricultural University, Xin kang Road 46 Ya'an, Sichuan 625000, P. R. China

Ye Ni yenicq@163.com Sichuan Agricultural University, Xin kang Road 46 Ya'an, Sichuan 625000, P. R. China

Cao San-jie csanjie@sicau.edu.cn Sichuan Agricultural University, Xin kang Road 46 Ya'an, Sichuan 625000, P. R. China

Wen Xin-tian xintian@sicau.edu.cnSichuan Agricultural University, Xin kang Road 46 Ya'an, Sichuan 625000, P. R. China

Huang Yong hyong601@163.com Sichuan Agricultural University, Xin kang Road 46 Ya'an, Sichuan 625000, P. R. China

Yan qi-gui yanqigui@126.com Sichuan Agricultural University, Xin kang Road 46 Ya'an, Sichuan 625000, P. R. China

[1]College of Veterinary Medicine, Sichuan Agricultural University, Yaan, Sichuan 625000, P. R. China

# Ye Ni as the joint first author

&Yan Qi-gui as the corresponding author

* To whom correspondence may be addressed: College of Veterinary Medicine, Sichuan Agricultural University, Yaan, Sichuan. Tel: +0835-28-824-23; Tel: +0835-28-824-23; E-mail:

24 yanqigui@126.com.

25

26 Running title: Differentially expressed miRNAs in goat ENA

27

28 **Abstract**

29 Enzootic nasal adenocarcinoma (ENA), an epithelial tumor induced in goats and sheep by
30 enzootic nasal tumor virus (ENTV), is a chronic, progressive, contact transmitted disease.
31 This study aimed to identify novel and differentially expressed miRNAs in the tumor and
32 para-carcinoma nasal tissues of Nanjiang yellow goats with ENA. Small RNA Illumina
33 high-throughput sequencing was used to construct a goat nasal miRNA library.

34 406 known miRNAs and 29 novel miRNAs were identified. A total of 116 miRNAs were
35 significantly differentially expressed in para-carcinoma nasal tissues and ENA; Target gene
36 prediction and functional analysis revealed that 6176 non-redundancy target genes, 1792
37 significant GO and 97 significant KEGG pathway for 121 miRNAs were predicted.

38 **Keywords:** MicroRNA; Enzootic Nasal Adenocarcinoma; Illumina High-throughput
39 Sequencing; Gene ontology; KEGG pathway

MicroRNAs (miRNAs) are endogenous, 21-24 nucleotide-long, non-coding RNAs that regulate gene expression in eukaryotes; however, some viruses also express miRNAs in host cells (Bartel 2004; Pfeffer et al. 2004; Filipowicz et al. 2005). MiRNAs are complementary to specific sequence motifs in the 3` untranslated regions (UTRs) of their target mRNAs and negatively regulate gene expression at the post-transcriptional level by inhibiting translation or promoting mRNA degradation, based on the degree of complementary base pairing between the miRNA and mRNA. MiRNAs regulate approximately 30% of genes in higher eukaryotic cells, including genes involved in development, metabolism, apoptosis, proliferation and viral defense(Kincaid and Sullivan 2012; Dong et al. 2013; Zhang et al. 2013; Wang and Kaufman 2014; Zhang et al. 2014; Bandiera et al. 2015; Lin et al. 2015). The earliest evidence for an association between miRNAs and cancer came from the study of chronic lymphocytic leukemia (CLL) (Calin et al. 2002). To date, more than 50% of miRNAs have been shown to be encoded in chromosome fragile sites that are often absent, amplified or rearranged in malignant tumor cells leading to dysregulated expression of miRNAs, and numerous miRNAs have been shown to play important roles in tumorigenesis (Calin et al. 2004). MiRNAs can act in a similar manner to oncogenes or tumor suppressor genes and have emerged as a novel type of regulatory factor in the epigenetic modification of gene expression. According to predictions in vertebrates, a single miRNA can regulate more than 400 target genes, forming complicated regulatory networks(Lewis et al. 2003; Landgraf et al. 2007; Ruby et al. 2007; Bartel 2009). Therefore, miRNAs have become a focus of cancer research in order to identify novel molecular methods for the diagnosis, prognostication and treatment of human cancer. Now researchers can directly obtain miRNA sequences and discover novel

62 miRNAs through utilize Illumina high-throughput sequencing technology(Ye et al. 2012).

63 Enzootic nasal adenocarcinoma (ENA) is an epithelial tumor caused by enzootic nasal
64 tumor virus (ENTV), and is a chronic, progressive, contact transmitted disease(Heras et al.
65 2003). With the exception of Australia and New Zealand, this disease has spread throughout
66 goats or sheep almost worldwide (Kawasako et al. 2005). ENA originates from the ethmoid
67 area of the nasal cavity either unilaterally or bilaterally, and the tumors are soft, whitish or
68 pinkish-red in color and can partially or completely obscure the nasal cavity(Walsh et al.
69 2010). Metastases to the regional lymph nodes, brain or other organs does not occur(Yi et al.
70 2010). So far, there are no effective methods for early diagnosis of ENA and the goats or
71 sheep can only be culled after symptoms appear. More seriously, as it is difficult to
72 distinguish between animals with a latent infection and healthy animals, the virus spreads
73 within herds, and can infect a large number of goats or sheep and threaten the entire
74 population.

75 There are currently 2581 human miRNAs in the miRbase (v21) database; however, there is
76 no public miRNA library of *Capra hircus* nasal tissues and there have been no reports of
77 miRNAs in ENA. To further complicate matters, attempts to establish a system of cultivating
78 ENTV *in vitro* have failed, which presents a significant obstacle to investigating the
79 immunological characteristics of ENTV and the mechanisms by which it promotes
80 tumorigenesis (De las Heras et al. 1995). Therefore, taking advantage of knowledge of the
81 roles of miRNAs in human cancer to research the miRNAs involved in ENA may not only
82 avoid the problem of cultivating ENTV *in vitro*, but also shifts the focus to the cells targeted
83 by ENTV - goat or sheep nasal epithelial cells - and may provide an alternative method for

84 investigating the tumorigenic effects of ENTV.

85 Using Illumina high-throughput sequencing technology to detect miRNAs expressed in the
86 tumor and para-carcinoma nasal tissues of Nanjiang yellow goats with ENA, we constructed
87 the first goat nasal tissue miRNA library. Furthermore, the target genes of the differentially
88 expressed miRNAs in ENA were predicted and their corresponding biological functions were
89 analyzed. This research may help to identify novel biomarkers for ENA, lays a foundation for
90 investigating the mechanism by which ENTV promotes tumorigenesis, and provides further
91 information on the role of miRNAs in cancer. Furthermore, as the sequences and roles of
92 miRNAs are well conserved, the findings of this study may also be relevant to human cancers
93 such as nasopharyngeal carcinoma.

94 **RESULTS**

95 **Capra hircus nasal tissue miRNA library**

96 High-throughput sequencing generated hundreds of millions of reads for each tissue. The
97 raw data (tag sequences and counts) have been submitted to Gene Expression Omnibus (GEO)
98 under series GSE65305. To estimate sequencing quality, the quality scores were analyzed
99 across all bases (Fig. 7). The lowest quality score was ≥ 30; therefore, the error rate was lower
100 than 0.1%. Reads including adaptor sequences, low quality sequences and sequences of
101 unqualified length were removed, and the remaining clean reads were aligned with the *Capra*
102 *hircus* genome in NCBI using Bowtie software to analyze the genomic distribution and
103 expression of small RNAs. The vast majority of clean reads (at least 84.75%) and unique
104 reads (at least 57.56%) mapped to the *Capra hircus* genome (Table 1).

105 Unique reads were blasted against the Rfam, RepBase, EST and miRBase databases, in the

106 order of known miRNAs > rRNAs > tRNAs > snRNAs > snoRNAs > repeat sequences,
107 which enabled each small RNA obtain a unique annotation. To exclude other RNAs, such as
108 tRNAs, rRNAs, snRNAs and snoRNAs, the remaining sequences were mapped to Denovo
109 prediction data sets and the *Capra hircus* genome to identify novel miRNAs. Using miRDeep
110 prediction (Friedländer et al. 2008) and RNAfold (Hofacker et al. 1994) software to analyze
111 secondary structure. A total of 435 sequences (29 novel miRNAs) were included in the
112 miRNA library. Table S1 displays the sequencing generated codes and corresponding *Capra*
113 *hircus* miRNAs or novel miRNA_id. As research into miRNAs in human cancer is
114 widespread, we blasted all goat miRNAs against the human miRNAs in miRBase v21 to
115 further understand their function. A total of 615 of the goat miRNAs had analogues in the
116 human miRNA datasets (Table S2).

117 **Identification of differentially expressed miRNAs in ENA**

118 A total of 435 miRNAs were identified in the ENA and para-carcinoma tissues. The table
119 S3 lists the expression of all miRNAs. The expression of 116 miRNAs was significantly
120 different in para-carcinoma tissues and ENA, of which 54 were downregulated and 60 were
121 upregulated in ENA. In addition, 2 miRNAs were only expressed in the para-carcinoma
122 tissues (Table S4). The majority of the fold change-$\log^2$ values ranged from 1 to 5.42;
123 chi-miR-133a-3p had the highest fold-change-$\log^2$ of at least 5.4-fold, and 65 miRNAs had
124 fold-change-$\log^2$ values of at least two-fold. Figure 8 indicates the differences in expression
125 of all 435 miRNAs between ENA and the para-carcinoma tissues.

126 **Functional analysis of differentially expressed target genes regulated by differentially**
127 **expressed miRNAs**

The Miranda algorithm indicated thousands of potential target genes for the 435 miRNAs. According to the total scores and predicted energies, the 6176 non-redundancy target genes of these 121 miRNA(116 significant expression miRNAs and 5 star miRNAs ) were selected, reflecting 15222 corresponding relationships between the differentially expressed miRNAs and their target genes. Table S5 shows the total stores, total energy, and protein-id and genomic location of predicted target genes.

The expression of these candidate target genes was assessed in the high throughput sequencing data obtained from the same ENA and para-cancerous tissue samples (data not shown; this data will be described in another article). A total of 175 mRNAs that were significantly differently expressed in ENA were selected for this analysis. Table S6 lists the differentially expressed miRNAs and their corresponding differentially expressed target genes. Table S7 summarizes the degree of regulation between the differentially expressed miRNAs and their differentially expressed target mRNAs.

**MiRNA-gene ontology network analysis of miRNA target genes**

Functional analysis was conducted on the mRNAs predicted as targets of the 435 differentially expressed miRNAs. A total of 9777 GO enrichments were identified, of which 1792 GO categories were significant ($P \leq 0.05$).The mRNA sequencing identified a total of 90 target genes corresponding to miRNAs with significantly decreased expression and 84 target genes corresponding to miRNA with significantly increased expression in tumor group. 472 significant GO enrichments exist in significant expression miRNA-mRNA network(Table S8). The target genes of the differentially expressed miRNAs were mainly involved in cell differentiation, MAP kinase activity, cell adhesion and angiogenesis; each of these pathways

may be implicated in the tumorigenic effect of ENTV. Figure 9 presents the ten most-enriched GO categories for the differentially expressed target genes of the differentially expressed miRNAs in ENA.

**Analysis of signaling pathways regulated by the miRNA target genes**

Signal transduction analysis was conducted on the mRNAs predicted as targets of the 435differentially expressed miRNAs, and 267 KEGG enrichments were identified of which 97 were significant ($P \leq 0.05$). The target genes of the differentially expressed miRNAs participate in pathways related to the signal transduction, specific types of cancer and immune system. Among significantly differently expressed miRNA, miRNA with increased expression in tumor group were involved in 83 significant signal transduction pathways(Table S9) , miRNA with reduced expression in tumor group were involved in 89 significant signal transduction pathways(Table S10). Figure 10 illustrates the ten most-enriched KEGG pathways for the differentially expressed target genes of the differentially expressed miRNAs in ENA.

**Quantitative RT-PCR validation of differentially expressed miRNAs**

We selected 9 of the key miRNAs that were significantly differently expressed in ENA including five miRNAs that featured in both the GO and KEGG pathway analyses and two novel miRNAs(NW_005102245.1_1433,NC_022308.1_285). The main functions of target genes regulated by these miRNAs are involved in cancer pathogenesis, virus infection, cell apoptosis and proliferation. As shown in Figure 11, qRT-PCR confirmed the expression of the nine miRNAs between ENA and the para-cancerous tissues with an increased sample size. The expression trend of eight miRNAs is in accord with Illumina High-Throughput

Sequencing, one miRNA(chi-miR-218) both in sequencing and qPCR verification have shown a down-expression in tumor group, but the down-expression multiple is different.

**Discussion**

ENTV, a betaretrovirus that infects sheep (ENTV-1) and goats (ENTV-2), is associated with neoplastic transformation of ethmoid turbinate epithelial cells and leads to ENA. The clinical symptoms of goats are a loss of appetite, extreme weight loss, dyspnea, rhinorrhea, and unilateral or bilateral nasal puffiness. The incidence of ENTV infection ranges from 5% to 15%, and once the clinical symptoms of ENA appear, almost all cases are fatal (Rings and Rojko 1985; De las Heras et al. 1991; Vitellozzi et al. 1993). High-throughput sequencing technology is gradually being used in animal and has provided some knowledge of goat miRNAs. Ji et al. (Ji et al. 2012) discovered 290 known miRNAs and 38 novel miRNAs in dairy goat mammary gland tissue and reported that miRNA-mediated regulation of gene expression occurs during early lactation. Hao et al. (Yu and Jun 2014)found that the expression of 64 miRNAs was reduced in the skin of a 70-day fetus relative to a lamb born at 2 weeks, with the expression of ten miRNAs decreasing more than 5-fold, which implies that miRNAs play an important role in maintaining normal skin function.

Cancer is a leading cause of morbidity and death in humans. Significant research has been conducted on miRNAs in human cancer, and miRNAs have been demonstrated to be directly involved in human nasopharyngeal carcinoma (NPC). For example, miR-29c, the miR-34 family, miR-143, miR-145 and miR-9 are downregulated in NPC, leading to increased expression of their target genes which influence the function and synthesis of extracellular matrix proteins, which in turn affects tumor invasion and metastasis, and activates the

194 TGF-Wnt, IP3 and VEGF signaling pathways (Sengupta et al. 2008; Chen et al. 2009). In
195 contrast, miR-200, the miR-17-92 cluster and miR-155 are upregulated in NPC, and miR-200
196 inhibits the migration and invasion of NPC cells by inhibiting the expression of *ZEB2* (zinc
197 finger E-box binding homeobox 2) and *CTNNB1*(catenin-β-like 1) (Xia et al. 2010). By
198 blasting the 435 miRNAs identified using high–throughput sequencing in this study against
199 the human miRNA datasets in miRBase, we found that hsa-miR-9, hsa-miR-34 and
200 hsa-miR-143 are significantly downregulated and hsa-miR-200 is significantly upregulated in
201 ENA. GO and KEGG pathway analysis revealed these miRNAs are involved in intracellular
202 signal transduction, the MAPK cascade and cell morphogenesis, among other processes.

203 Our study found according to the percentage, the top five signaling pathways are MAPK
204 signaling pathway、Pathways in cancer、PI3K-Akt signaling pathway、Ras signaling pathway
205 and Viral carcinogenesis. Kano et al. (Kano et al. 2010) and Chiyomaru et al. (Chiyomaru et
206 al. 2010) found that miR-133a was significantly inhibited human esophageal squamous cell
207 cancer and the invasion of bladder cancer cell. Iorio (Iorio et al. 2005) found that expression
208 of miR-133a significantly reduced during the progression of breast cancer. Our results also
209 reveal the expression of miR-133a-3p was at least 5-fold lower in ENA compared to
210 para-carcinoma nasal tissues. These results suggest that miR-133a-3p may regulate the
211 expression of oncogenes and inhibit tumorigenesis. KEGG analysis displayed that the target
212 genes of miR-133a-3p are involved in tumor biology at multiple nodes, such as regulation of
213 cell differentiation, apoptosis, signal transduction and cell adhesion, invasion and migration.
214 In esophageal squamous cell carcinoma and bladder cancer, miR-133a targets fascin
215 actin-bundling protein 1(*FSCN1* ) to regulate cancer cell invasion, migration and proliferation

(Iorio et al. 2005; Kano et al. 2010). However, in this study we identified that serine/threonine-protein kinase B-raf (*BRAF)* as chi- miR-133a-3p, chi-miR-145-5p,chi-miR-146a/200a and two novel miRNA(NC-022308.1-260 、NC-022294.1-874) target gene which acts upstream regulatory factor in RAS-RAF-MEK-ERK. Sustained activation of BRAF will lead to cell deterioration and excessive proliferation(Ji et al. 2007). In addition, the miR-133a-3p target genes:*MDS1* and *EVI1* complex (*MECOM*) may also play a significant role in pathways related to cancer. In chronic myeloid leukemia *(CML)*, expression of the oncogene *MECOM* correlates with progression. The tyrosine kinase catalytic activity of the oncoprotein BCL-ABL1 regulates *MECOM* expression, and conversely MECOM partially mediates BCR-ABL1 activity (Roy et al. 2012); BCR-ABL1 activates the PI3K, MAPK and JAK-STAT signal transduction pathways (Pendergast et al. 1993; Carlesso et al. 1996; Skorski et al. 1997) to promote abnormal proliferation, differentiation, transformation and survival in myeloid cells (Smith et al. 2003). However, forkhead box O *(FoxO*) as the intersection of PI3K and RAS signaling pathway can inhibit cell proliferation and induce cell cycle stop. The activation of the PI3K signaling pathway inhibits the activity of the FoxO transcription factor(Schmidt et al. 2002; Martínez-Gac et al. 2004),which increase the chances of tumor formation. Further study is required to determine if *MECOM* and BCR-ABL1 play a role in the pathogenesis of ENA.

miR-148a is an oncogene that is upregulated in hepatocellular carcinoma cells (*HCC*) and enhances cell proliferation, migration, invasion and stimulates the epithelial to mesenchymal transition *(EMT)* by targeting tumor suppressor gene: phosphatase and tensin homolog (*PTEN)*(Yuan et al. 2012). However, *PTEN* was not identified as a target of miR-148a in this

study. Its predicted targets were the transforming growth factor β receptor associated protein 1( *TGFβRAP1)* which can specifically combine with the receptor of transforming growth factor β(*TGFβ*),and then help to realize the biological function of TGFβ(Chen et al. 1995).TGFβ can inhibit cells growth in malignant tumor such as head and neck squamous cancer, colon cancer, breast cancer(Arteaga et al. 1990; Wu et al. 1992; Briskin et al. 1995).The present studies have pointed out that the expression of TGFβ in nasopharyngeal phosphorus tumor generally weakened or even disappear, but the adjacent epithelium have stronger expression(Bin et al. 1999). The expression of miR-148a-3p was at least 2.5-fold higher in ENA compared to para-carcinoma nasal tissues. Influenced by miR-148-3p expression, *TGFβRAP1* will drop, which will affect the signal pathway of TGFβ and make the cancer cell reduction or loss of ability to react to TGFβ, finally, the tumor cells escape from negative growth regulation of TGFβ.Although this is our speculation, but we believe there is a link between them.

## Conclusions

This study provides a solid basis for further research and highlights a number of miRNAs and genes that may be involved in the pathogenesis of ENA. This study of miRNAs in ENA may also provide useful information for basic research into human cancer. In future studies, we aim to confirm the function of the candidate miRNAs in nasal cells. In addition, we hope that these studies may provide some clues to help establish a method for cultivating ENTV *in vitro*.

## Methods

### Ethics Statement

This study was carried out in strict accordance with the Guidelines for Experimental Animals of the Ministry of Science and Technology (revised in 2004; Beijing, China) and was approved by the Institutional Animal Care and Use Ethics Committee of Sichuan Agricultural University, NO. SYXK (Chuan) 2014-187.

**Animals and tissue samples**

Eight goats (3a-4a)infected by ENTV under natural conditions at a farm in Sichuan were quarantined and transported to Sichuan Agricultural University laboratory animal center, and grew up the center. After slaughter, tumor and para-carcinoma nasal tissues were collected, frozen rapidly in liquid nitrogen and stored at -80°C. After pathological analysis, the samples from three Nanjiang yellow goats whose nasal passages were unilaterally blocked by tumors were selected for high-throughput sequencing. The nasal tumors in these animals were poorly differentiated (i.e., at the same state of differentiation) with no tumor cell infiltration in the matched para-carcinoma tissues.

**Preparation of samples for sequencing and qPCR**

Samples of cDNA from the tumor tissues (numbers S1, S3, S5) and matched para-carcinoma tissues (numbers S2, S4, S6) of the three animals described above were shipped on dry ice to Jing Neng Bio-Technology corporation (Shanghai, China) for high-throughput sequencing. Briefly, total RNA was extracted from the tissues using RNAzol RT RNA Isolation Reagent (GeneCopoela, Rockville, MD, USA) according to the manufacturer's protocol. The RNA concentrations were determined using a Smart Specplus Spectrophotometer (Bio-Rad, Hercules, CA, USA) and the integrity of the total RNA samples was verified by polyacrylamide gel electrophoresis (PAGE). The All-In-One miRNA

qRT-PCR Detection Kit (GeneCopoela) was used to add poly(A) tails to the miRNAs in the total RNA samples and M-MLV reverse transcriptase was used to synthesize cDNA according to the manufacturer's instructions. Each reaction mixture contained 5 μL of 5x reaction buffer, 1 μL RTase Mix, 1 μL of 2.5 U/μL PolyA Polymerase, 2 μg total RNA and RNase-/DNase-free H2O to 25 μL, and was incubated at 37°C for 1 h and then at 85°C for 5 min to inactivate the enzyme.

**Analysis of sequence data and creation of miRNA library**

Single-read 50 bp sequencing was adopted for high-throughput sequencing. Illumina CASAVA software was used to convert the original data image files into sequence files, and FastQC statistical software was used to evaluate the quality of the data. Primer, adaptor and low quality sequences were excluded and 15-40 base sequences meeting the length and quality requirements were selected as clean reads of reliable quality for further analysis(Figure 1-6). Total clean reads from each individual sample were aligned with the Capra hircus genome in NCBI (ftp://ftp.ncbi.nlm.nih.gov/genomes/Capra_hircus) using Bowtie software (Langmead et al. 2009)(http://bowtie-bio.sourceforge.net/index.shtml) , and then blasted against the Rfam (http://www.sanger.ac.uk/resources/databases/rfam.html) , RepBase (http://www.girinst.org/repbase/) , EST (http://www.ncbi.nlm.nih.gov/nucest/) and miRBase (http://www.mirbase.org/) databases. Sequence alignment was set to allow only a single base mismatch, and the results were sorted in the order of known miRNAs > rRNAs > tRNAs > snRNAs > snoRNAs > repeat, respectively, which enabled each small RNA to obtain a unique annotation. The remaining sequences were mapped to Denovo prediction data sets (Bonneau et al. 2006)and the *Capra hircus* genome to exclude known non-miRNA

304 sequences (such as tRNAs, rRNAs, snRNAs and snoRNAs) and identify novel miRNAs.
305 MiRDeep (Friedländer et al. 2008)and RNAfold (Hofacker et al. 1994)were used to predict
306 miRNA precursor sequences, star miRNAs and mature miRNAs, and then the energetic
307 stability, position and read frequencies for each potential miRNA precursor were computed
308 using miRDeep according to the compatibility of energetic stability, positions, frequencies of
309 reads. Ultimately, a *Capra hircus* nasal tissue miRNA library was created by combining the
310 sequencing data from all six samples.

311 **Identification of differentially expressed miRNAs in ENA**

312 The sequences in each sample were compared with the miRNA library established in this
313 study by assessing the numbers of transcripts per million (TPM). TPM was calculated as
314 (numbers of each miRNA matched to total reads)/(number total reads) x $10^6$. TPM is an
315 indicator of the quantity of miRNA expression per million match paired sequences. The total
316 numbers of matched pair reads were used in the normalized numerical expression algorithm
317 to calculate miRNA expression. DESeq (Anders and Huber 2010)software was used to
318 identify differentially expressed miRNAs between the para-carcinoma tissues (S2 , S4, S6)
319 and ENA (S1, S3, S5) on the basis of a fold-change greater than or equal to two and *P*-value ≤
320 0.05.

321 **Prediction and analysis of miRNA target genes**

322 The Miranda algorithm (Enright et al. 2004)was used to predict the target genes of the
323 miRNAs that were differently expressed in ENA. The threshold parameters for predicting
324 miRNA target genes were a total score ≥ 150, ΔG ≤ -30 kcal/mol, and strict 5` seed pairing.
325 The pathways these candidate target genes are involved in was analyzed by functional

326 annotation utilizing the NCBI, KEGG(http://www.genome.jp/kegg/)(Kanehisa et al. 2011)
327 and GO(http://geneontology.org/) (Carbon et al. 2009) databases. Additionally,
328 high-throughput sequencing allowed the mRNA expression of all of the potential target genes
329 to be analyzed in the same samples (data not shown); therefore, GO and KEGG analyses
330 could be conducted on the differentially expressed target genes of the differentially expressed
331 miRNAs. GO annotation and enrichment analysis was performed for three gene ontologies:
332 molecular function, cellular components and biological processes. The following formula was
333 used to calculate the *P*-values:
334

$$P = 1 - \sum_{i=0}^{m-1} \frac{\binom{M}{i}\binom{N-M}{n-i}}{\binom{N}{n}}$$

335
336 where *N* is the number of genes with GO/KEGG annotations; *n* is the number of target gene
337 candidates in *N*; *M* is the number of genes that annotated to a certain GO term/pathway, and *m*
338 is the number of target gene candidates in *M*. GO terms and KEGG pathways with a corrected
339 *P*-value $\leq 0.5$ were regarded as significantly enriched.
340 **Validation of the expression of key differentially expressed miRNAs**
341 Key miRNAs that were identified in all of the analyses described above were quantified
342 in ENA and para-carcinoma tissue samples from five goats with ENA whose nasal passages
343 were unilaterally blocked by tumors. Total RNA was isolated and reverse transcribed as
344 described above, then the cDNA products were diluted 5-fold with sterile $H_2O$ and subjected
345 to quantitative real-time PCR (qPCR) using the All-In-One miRNA qRT-PCR Detection Kit
346 (GeneCopoela) with U6 snRNA and *GAPDH* as internal references. Each reaction contained

10 µL of 2x All-in-One qPCR Mix, 2 µL All-in-One miRNA qPCR Primer (2 µM; prepared by Life Technologies, Shanghai, China), 2 µL Universal Adaptor qPCR Primer (2 µM), 2 µL first-strand cDNA and 4 µL double distilled water. The cycling conditions were 95°C for 10 min, 40 cycles of 95°C for 10 s, 60°C for 20 s and 72°C for 20 s, followed by melting curve analysis. Relative quantification was performed using the $2^{-\Delta\Delta Ct}$ method (Livak and Schmittgen 2001), and *t*-tests were used to examine the significance of the differences in expression between the para-carcinoma tissues and ENA.

## Availability of data and material

The raw data (tag sequences and counts) have been submitted to Gene Expression Omnibus (GEO) under series GSE65305.

## Abbreviations

**miRNAs**: MicroRNAs **ENA:** Enzootic nasal adenocarcinoma **ENTV**: Enzootic nasal tumor virus **GO:** Gene Ontology **KEGG:** Kyoto Encyclopedia of Genes and Genomes **RNA**：ribonucleic acid **UTRs**：untranslated regions **CLL**：chronic lymphocytic leukemia **PAGE**：polyacrylamide gel electrophoresis **rRNAs**：ribosomal RNAs **tRNAs**：transfer RNAs **snRNAs**：Small nuclear RNAs **snoRNAs**：Small nucleolar RNAs **TPM**：transcripts per million **qPCR**：quantitative real-time PCR **GAPDH**：glyceraldehyde-3-phosphate dehydrogenase **GEO**：Gene Expression Omnibus **NPC**：nasopharyngeal carcinoma

## Declarations

## Acknowledgments

The skillful technical assistance of Shanghai Genergy Bio-Corporation is gratefully acknowledged.

## Competing interest

The authors declare no financial conflict of interest

## Author Contributions

All authors have read and approved of the submission of the manuscript. Conceived and designed the experiments: YQG CSJ WXT. Performed the experiments: WB YE. Analyzed the data: WB YE HY. Contributed reagents/materials/analysis tools: YQG WB YE.Wrote the paper: WB YN.

## References

Anders S, Huber W. 2010. Differential expression analysis for sequence count data. *Genome biol* **11**(10): R106.

Arteaga C, Coffey Jr R, Dugger T, McCutchen C, Moses H, Lyons R. 1990. Growth stimulation of human breast cancer cells with anti-transforming growth factor beta antibodies: evidence for negative autocrine regulation by transforming growth factor beta. *Cell growth & differentiation: the molecular biology journal of the American Association for Cancer Research* **1**(8): 367-374.

Bandiera S, Pfeffer S, Baumert TF, Zeisel MB. 2015. miR-122–a key factor and therapeutic target in liver disease. *Journal of hepatology* **62**(2): 448-457.

Bartel DP. 2004. MicroRNAs: genomics, biogenesis, mechanism, and function. *cell* **116**(2): 281-297.

-. 2009. MicroRNAs: target recognition and regulatory functions. *Cell* **136**(2): 215-233.

Bin L, Hu C, Zhan F. 1999. [The expression in situ of transforming growth factor beta s, their receptors and TGF beta-receptor interacting protein-1 in nasopharygneal carcinoma]. *Zhonghua er bi yan hou ke za zhi* **34**(4): 210-212.

Bonneau R, Reiss DJ, Shannon P, Facciotti M, Hood L, Baliga NS, Thorsson V. 2006. The Inferelator: an algorithm for learning parsimonious regulatory networks from systems-biology data sets de novo. *Genome biology* **7**(5): R36.

Briskin KB, Fady C, Mickel RA, Wang M, Lichtenstein A. 1995. Inhibition of head and neck squamous cell carcinoma cell lines by transforming growth factor-β. *Otolaryngology-Head and Neck Surgery* **112**(6): 728-734.

Calin GA, Dumitru CD, Shimizu M, Bichi R, Zupo S, Noch E, Aldler H, Rattan S, Keating M, Rai K. 2002. Frequent deletions and down-regulation of micro-RNA genes miR15 and miR16 at 13q14 in chronic lymphocytic leukemia. *Proceedings of the National Academy of Sciences* **99**(24): 15524-15529.

Calin GA, Sevignani C, Dumitru CD, Hyslop T, Noch E, Yendamuri S, Shimizu M, Rattan S, Bullrich F, Negrini M. 2004. Human microRNA genes are frequently located at fragile sites and genomic regions involved in cancers. *Proceedings of the National Academy of Sciences of the United States of America* **101**(9): 2999-3004.

405 Carbon S, Ireland A, Mungall CJ, Shu S, Marshall B, Lewis S. 2009. AmiGO: online access to ontology
406 and annotation data. *Bioinformatics* **25**(2): 288-289.
407 Carlesso N, Frank DA, Griffin JD. 1996. Tyrosyl phosphorylation and DNA binding activity of signal
408 transducers and activators of transcription (STAT) proteins in hematopoietic cell lines
409 transformed by Bcr/Abl. *The Journal of experimental medicine* **183**(3): 811-820.
410 Chen H, Chen G, Chen Y, Liao W, Liu C, Chang K, Chang Y, Chen S. 2009. MicroRNA deregulation and
411 pathway alterations in nasopharyngeal carcinoma. *British journal of cancer* **100**(6):
412 1002-1011.
413 Chen R-H, Miettinen PJ, Maruoka EM, Choy L, Derynck R. 1995. A WD-domain protein that is
414 associated with and phosphorylated by the type II TGF-β receptor.
415 Chiyomaru T, Enokida H, Tatarano S, Kawahara K, Uchida Y, Nishiyama K, Fujimura L, Kikkawa N, Seki N,
416 Nakagawa M. 2010. miR-145 and miR-133a function as tumour suppressors and directly
417 regulate FSCN1 expression in bladder cancer. *British journal of cancer* **102**(5): 883-891.
418 De las Heras M, de Jalon JG, Minguijon E, Gray E, Dewar P, Sharp J. 1995. Experimental transmission of
419 enzootic intranasal tumors of goats. *Veterinary Pathology Online* **32**(1): 19-23.
420 De las Heras M, de Jalon JG, Sharp J. 1991. Pathology of enzootic intranasal tumor in thirty-eight goats.
421 *Veterinary Pathology Online* **28**(6): 474-481.
422 Dong H, Lei J, Ding L, Wen Y, Ju H, Zhang X. 2013. MicroRNA: function, detection, and bioanalysis.
423 *Chemical reviews* **113**(8): 6207-6233.
424 Enright AJ, John B, Gaul U, Tuschl T, Sander C, Marks DS. 2004. MicroRNA targets in Drosophila.
425 *Genome biology* **5**(1): R1-R1.
426 Filipowicz W, Jaskiewicz L, Kolb FA, Pillai RS. 2005. Post-transcriptional gene silencing by siRNAs and
427 miRNAs. *Current opinion in structural biology* **15**(3): 331-341.
428 Friedländer MR, Chen W, Adamidi C, Maaskola J, Einspanier R, Knespel S, Rajewsky N. 2008.
429 Discovering microRNAs from deep sequencing data using miRDeep. *Nature biotechnology*
430 **26**(4): 407-415.
431 Heras M, Ortin A, Cousens C, Minguijon E, Sharp J. 2003. Enzootic nasal adenocarcinoma of sheep and
432 goats. *Jaagsiekte Sheep Retrovirus and Lung Cancer*: 201-223.
433 Hofacker IL, Fontana W, Stadler PF, Bonhoeffer LS, Tacker M, Schuster P. 1994. Fast folding and
434 comparison of RNA secondary structures. *Monatshefte für Chemie/Chemical Monthly* **125**(2):
435 167-188.
436 Iorio MV, Ferracin M, Liu C-G, Veronese A, Spizzo R, Sabbioni S, Magri E, Pedriali M, Fabbri M,
437 Campiglio M. 2005. MicroRNA gene expression deregulation in human breast cancer. *Cancer*
438 *research* **65**(16): 7065-7070.
439 Ji H, Wang Z, Perera SA, Li D, Liang M-C, Zaghlul S, McNamara K, Chen L, Albert M, Sun Y. 2007.
440 Mutations in BRAF and KRAS converge on activation of the mitogen-activated protein kinase
441 pathway in lung cancer mouse models. *Cancer Research* **67**(10): 4933-4939.
442 Ji Z, Wang G, Xie Z, Zhang C, Wang J. 2012. Identification and characterization of microRNA in the dairy
443 goat (Capra hircus) mammary gland by Solexa deep-sequencing technology. *Molecular*
444 *biology reports* **39**(10): 9361-9371.
445 Kanehisa M, Goto S, Sato Y, Furumichi M, Tanabe M. 2011. KEGG for integration and interpretation of
446 large-scale molecular data sets. *Nucleic acids research*: gkr988.
447 Kano M, Seki N, Kikkawa N, Fujimura L, Hoshino I, Akutsu Y, Chiyomaru T, Enokida H, Nakagawa M,
448 Matsubara H. 2010. miR-145, miR-133a and miR-133b: Tumor-suppressive miRNAs target

FSCN1 in esophageal squamous cell carcinoma. *International journal of cancer* **127**(12): 2804-2814.

Kawasako K, Okamoto M, Kurosawa T, Nakade T, Kirisawa R, Miyashou T, Komine M, Go T, Imazu S, Takeuchi N. 2005. Enzootic intranasal tumour virus infection in apparently healthy sheep in Japan. *The Veterinary Record* **157**(4): 118.

Kincaid RP, Sullivan CS. 2012. Virus-encoded microRNAs: an overview and a look to the future. *PLoS Pathog* **8**(12): e1003018.

Landgraf P, Rusu M, Sheridan R, Sewer A, Iovino N, Aravin A, Pfeffer S, Rice A, Kamphorst AO, Landthaler M. 2007. A mammalian microRNA expression atlas based on small RNA library sequencing. *Cell* **129**(7): 1401-1414.

Langmead B, Trapnell C, Pop M, Salzberg SL. 2009. Ultrafast and memory-efficient alignment of short DNA sequences to the human genome. *Genome Biol* **10**(3): R25.

Lewis BP, Shih I-h, Jones-Rhoades MW, Bartel DP, Burge CB. 2003. Prediction of mammalian microRNA targets. *Cell* **115**(7): 787-798.

Lin MV, King LY, Chung RT. 2015. Hepatitis C virus-associated cancer. *Annual Review of Pathology: Mechanisms of Disease* **10**: 345-370.

Livak KJ, Schmittgen TD. 2001. Analysis of Relative Gene Expression Data Using Real-Time Quantitative PCR and the 2< sup>− ΔΔCT</sup> Method. *methods* **25**(4): 402-408.

Martínez-Gac L, Marqués M, García Z, Campanero MR, Carrera AC. 2004. Control of cyclin G2 mRNA expression by forkhead transcription factors: novel mechanism for cell cycle control by phosphoinositide 3-kinase and forkhead. *Molecular and cellular biology* **24**(5): 2181-2189.

Pendergast AM, Quilliam LA, Cripe LD, Bassing CH, Dai Z, Li N, Batzer A, Rabun KM, Der CJ, Schlessinger J. 1993. BCR-ABL-induced oncogenesis is mediated by direct interaction with the SH2 domain of the GRB-2 adaptor protein. *Cell* **75**(1): 175-185.

Pfeffer S, Zavolan M, Grässer FA, Chien M, Russo JJ, Ju J, John B, Enright AJ, Marks D, Sander C. 2004. Identification of virus-encoded microRNAs. *Science* **304**(5671): 734-736.

Rings D, Rojko J. 1985. Naturally occurring nasal obstructions in 11 sheep. *The Cornell veterinarian* **75**(2): 269-276.

Roy S, Jørgensen HG, Roy P, Abed El Baky M, Melo JV, Strathdee G, Holyoake TL, Bartholomew C. 2012. BCR-ABL1 tyrosine kinase sustained MECOM expression in chronic myeloid leukaemia. *British journal of haematology* **157**(4): 446-456.

Ruby JG, Stark A, Johnston WK, Kellis M, Bartel DP, Lai EC. 2007. Evolution, biogenesis, expression, and target predictions of a substantially expanded set of Drosophila microRNAs. *Genome research* **17**(12): 1850-1864.

Schmidt M, de Mattos SF, van der Horst A, Klompmaker R, Kops GJL, Lam EW-F, Burgering BM, Medema RH. 2002. Cell cycle inhibition by FoxO forkhead transcription factors involves downregulation of cyclin D. *Molecular and cellular biology* **22**(22): 7842-7852.

Sengupta S, den Boon JA, Chen I-H, Newton MA, Stanhope SA, Cheng Y-J, Chen C-J, Hildesheim A, Sugden B, Ahlquist P. 2008. MicroRNA 29c is down-regulated in nasopharyngeal carcinomas, up-regulating mRNAs encoding extracellular matrix proteins. *Proceedings of the National Academy of Sciences* **105**(15): 5874-5878.

Skorski T, Bellacosa A, Nieborowska-Skorska M, Majewski M, Martinez R, Choi JK, Trotta R, Wlodarski P,

Perrotti D, Chan TO. 1997. Transformation of hematopoietic cells by BCR/ABL requires activation of a PI-3k/Akt-dependent pathway. *The EMBO journal* **16**(20): 6151-6161.

Smith DL, Burthem J, Whetton AD. 2003. Molecular pathogenesis of chronic myeloid leukaemia. *Expert reviews in molecular medicine* **5**(27): 1-27.

Vitellozzi G, Mughetti L, Palmarini M, Mandara M, Mechelli L, Sharp J, Manocchio I. 1993. Enzootic intranasal tumour of goats in Italy. *Journal of Veterinary Medicine, Series B* **40**(1-10): 459-468.

Walsh SR, Linnerth-Petrik NM, Laporte AN, Menzies PI, Foster RA, Wootton SK. 2010. Full-length genome sequence analysis of enzootic nasal tumor virus reveals an unusually high degree of genetic stability. *Virus research* **151**(1): 74-87.

Wang M, Kaufman RJ. 2014. The impact of the endoplasmic reticulum protein-folding environment on cancer development. *Nature Reviews Cancer* **14**(9): 581-597.

Wu S, Theodorescu D, Kerbel RS, Willson J, Mulder KM, Humphrey LE, Brattain MG. 1992. TGF-beta 1 is an autocrine-negative growth regulator of human colon carcinoma FET cells in vivo as revealed by transfection of an antisense expression vector. *The Journal of cell biology* **116**(1): 187-196.

Xia H, Ng SS, Jiang S, Cheung WK, Sze J, Bian X-W, Kung H-f, Lin MC. 2010. miR-200a-mediated downregulation of ZEB2 and CTNNB1 differentially inhibits nasopharyngeal carcinoma cell growth, migration and invasion. *Biochemical and biophysical research communications* **391**(1): 535-541.

Ye L, Su X, Wu Z, Zheng X, Wang J, Zi C, Zhu G, Wu S, Bao W. 2012. Analysis of differential miRNA expression in the duodenum of Escherichia coli F18-sensitive and-resistant weaned piglets. *PloS one* **7**(8): e43741.

Yi G, KaiYu W, QiGui Y, YingDong Y, DeFang C, JinLu H. 2010. Pathomorphologic observation of enzootic intranasal adenocarcinoma in Nanjiang yellow goats. *Chinese Journal of Veterinary Science* **30**(8): 1095-1097.

Yu H, Jun Y. 2014. Analysis of miRNAs between 70 Days Fetal and Lamb Skin. *Biotechnology* **5**: 018.

Yuan K, Lian Z, Sun B, Clayton MM, Ng IO, Feitelson MA. 2012. Role of miR-148a in hepatitis B associated hepatocellular carcinoma. *PLoS One* **7**(4): e35331.

Zhang X-D, Wang Y, Ye L-H. 2014. Hepatitis B virus X protein accelerates the development of hepatoma. *Cancer biology & medicine* **11**(3): 182-190.

Zhang X, Daucher M, Armistead D, Russell R, Kottilil S. 2013. MicroRNA expression profiling in HCV-infected human hepatoma cells identifies potential anti-viral targets induced by interferon-α. *PLoS One* **8**(2): e55733.

526 **Supporting Information**

527 **Figure1-6 . Reads length distribution statistical of S1-6**

528 **Figure 7.** Base quality distribution in each cycle.

529

530 **Figure 8.** Relative expression of miRNAs in ENA and para-cancerous tissues. The *x*- and

531 *y*-axes indicate the mean TPM expression levels of the miRNAs in each tissue. The red circles

532 represent miRNAs with a fold change ≥ 2; green circles represent miRNAs with a fold change

533 ≤ 2; the points on the dotted line represent miRNAs with a fold change = 2. Fold changes

534 were calculated as the mean miRNA TPM in ENA/mean miRNA TPM in para-cancerous

535 tissues.

536

537 **Figure 9.** The ten most-enriched GO categories of the differentially expressed target genes of

538 the differentially expressed miRNAs.

539 (PDF)

540

541 **Figure 10**. The ten most-enriched signaling pathways of the differentially expressed target

542 genes of the differentially expressed miRNAs.

543 (PDF)

544

545 **Figure 11**.qRT-PCR validation of the identified miRNAs using Illumina sequencing

546 technology. Real-time RT-PCR analysis of nine miRNAs in the tumour and para-carcinoma

547 tissues from 5 goats with ENA. Relative quantification was assessed using the $2^{-\Delta\Delta Cq}$ method

548 and was normalized to *U6* and *GAPDH*. $2^{-\Delta\Delta Ct}$ Means ± SE relative expression levels are

549 presented. * represents $p<0.05$,** represents $p<0.01$.

550

551 **Table 1.** Clean reads and unique reads from the ENA and para-cancerous tissues that mapped

552 to the *Capra hircus* genome.

553

554 **Table S1**. The miRNAs expressed in samples detected by Illumina sequencing.

555 (XLSX)

556

557 **Table S2.** Blast results of all miRNAs against human miRNAs in miRBase v21.

558 (XLS)

559

560 **Table S3.** The expression of miRNAs in ENA and para-cancerous tissues.

561 (XLS)

562

563 **Table S4.** Significantly differentially expressed miRNAs in ENA.

564 (.XLSX)

565 Positive FoldChange_Log2 indicates upregulation in ENA relative to the para-cancerous

566 tissues; a negative FoldChange_Log2 indicates downregulation in ENA relative to the

567 para-cancerous tissues; inf indicates no expression in para-cancerous tissues; -inf indicates no

568 expression in ENA.

569

570

571 **Table S5.** Predicted target genes of the differently expressed miRNAs in ENA.

572 (XLS)

573

574 **Table S6.** Differentially expressed miRNAs and their differentially expressed target genes in

575 ENA.

576 (XLS)

577

578 **Table S7.** Node attributes of the differentially expressed miRNAs and their differentially

579 expressed target genes in ENA.

580 (XLSX)

581

582 **Table S8.** Significantly enriched gene ontology categories the differentially expressed target

583 genes of the differentially expressed miRNAs.

584 (XLS)

585

586 **Table S9.** Significantly enriched signaling pathways (m=83)of gene targets of the

587 significantly increased miRNAs in ENA.

588 (XLS)

589

590 **Table S10**. Significantly enriched signaling pathways (m=89)of gene targets of the

591 significantly reduced miRNAs in ENA.

592 (XLS)

593

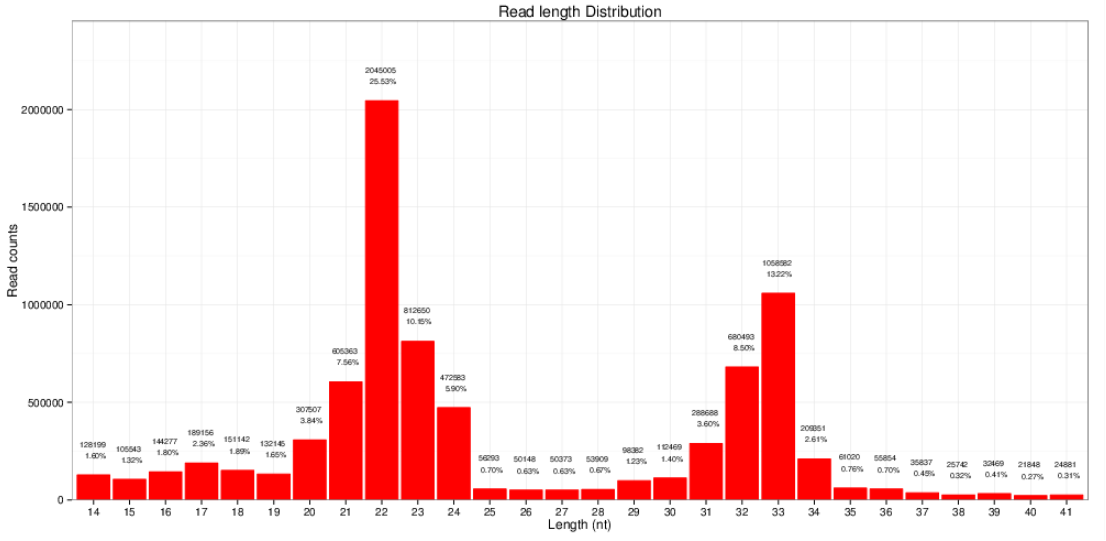


**Fig .1 Reads length distribution statistical of S1**

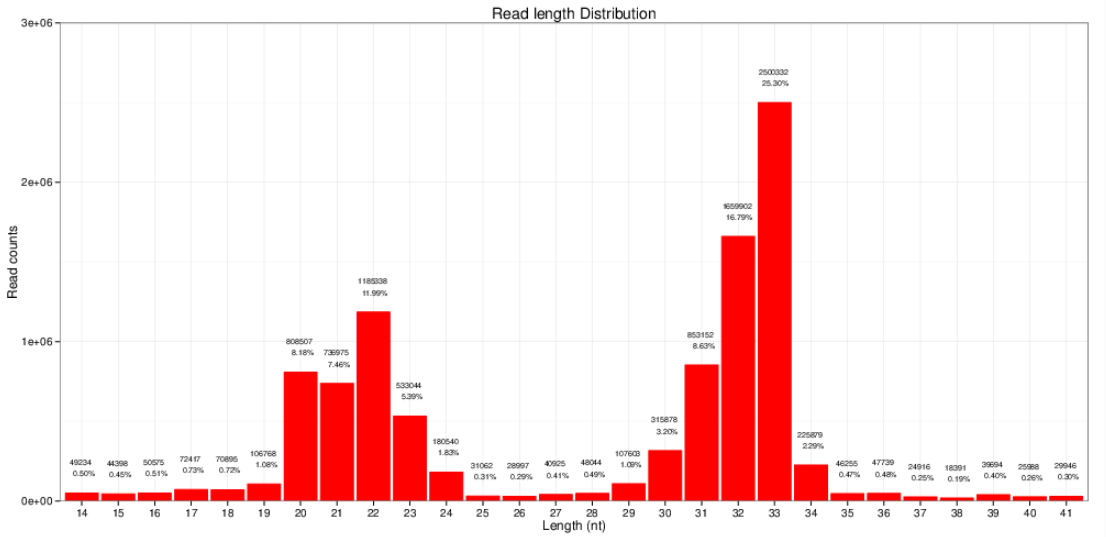


**Fig .2 Reads length distribution statistical of S2**

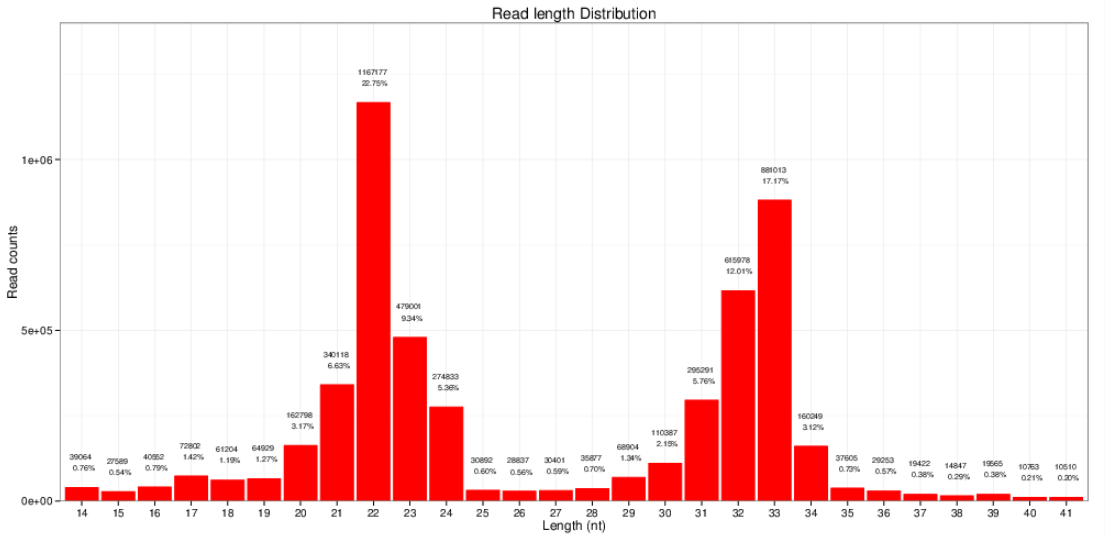


**Fig .3 Reads length distribution statistical of S3**

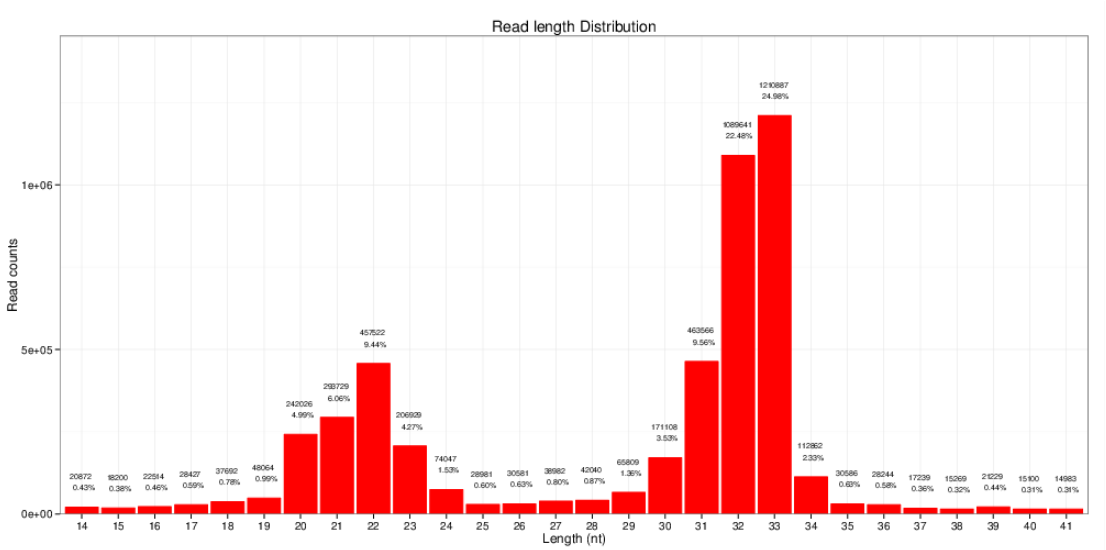


**Fig .4 Reads length distribution statistical of S4**

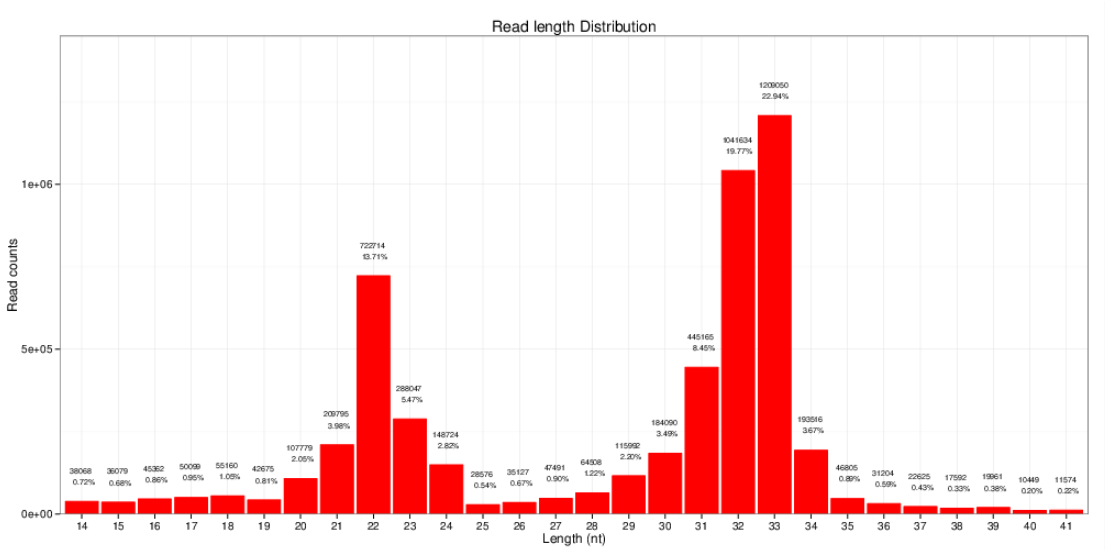


**Fig .5 Reads length distribution statistical of S5**

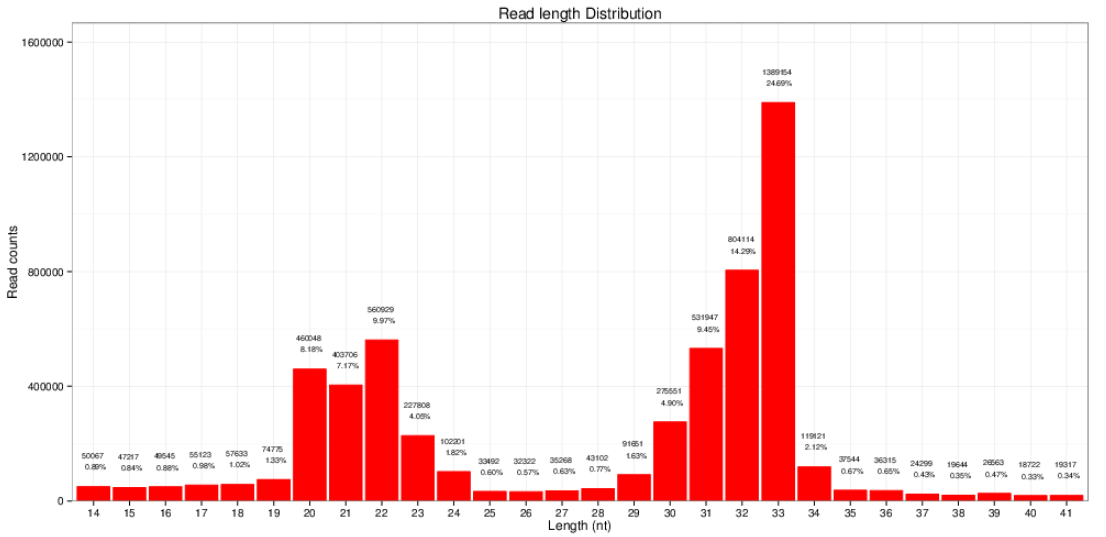


**Fig .6 Reads length distribution statistical of S6**

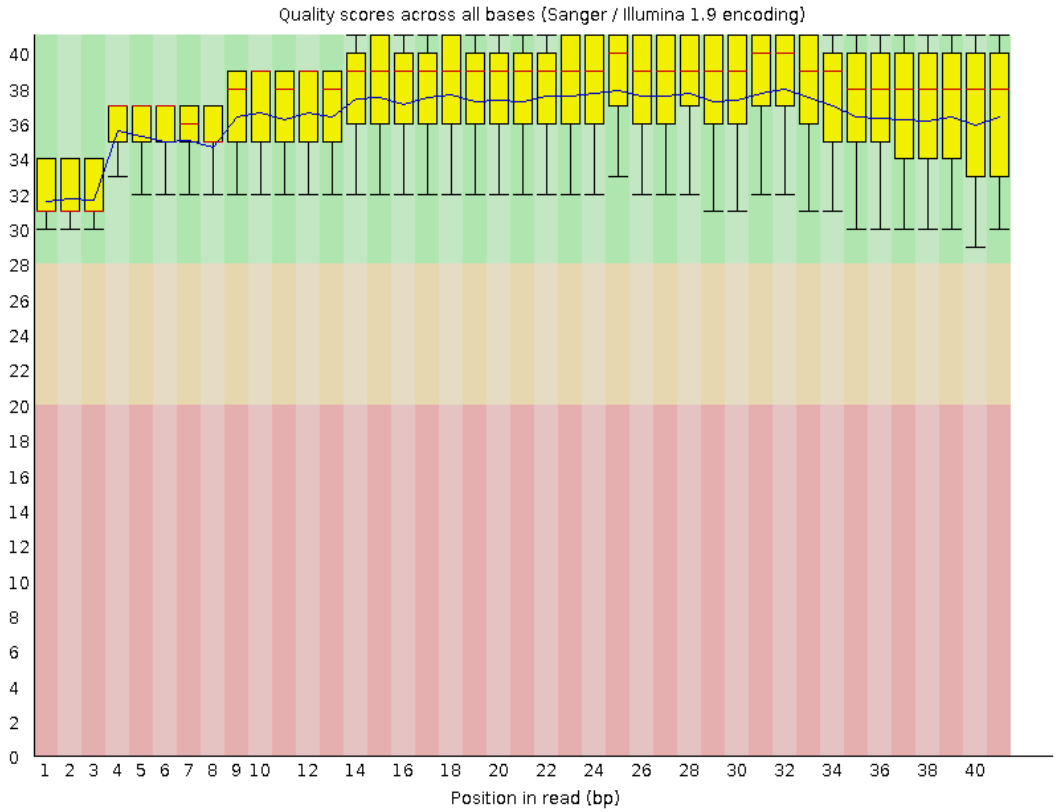


**Fig .7 Base quality distribution in each cycle**

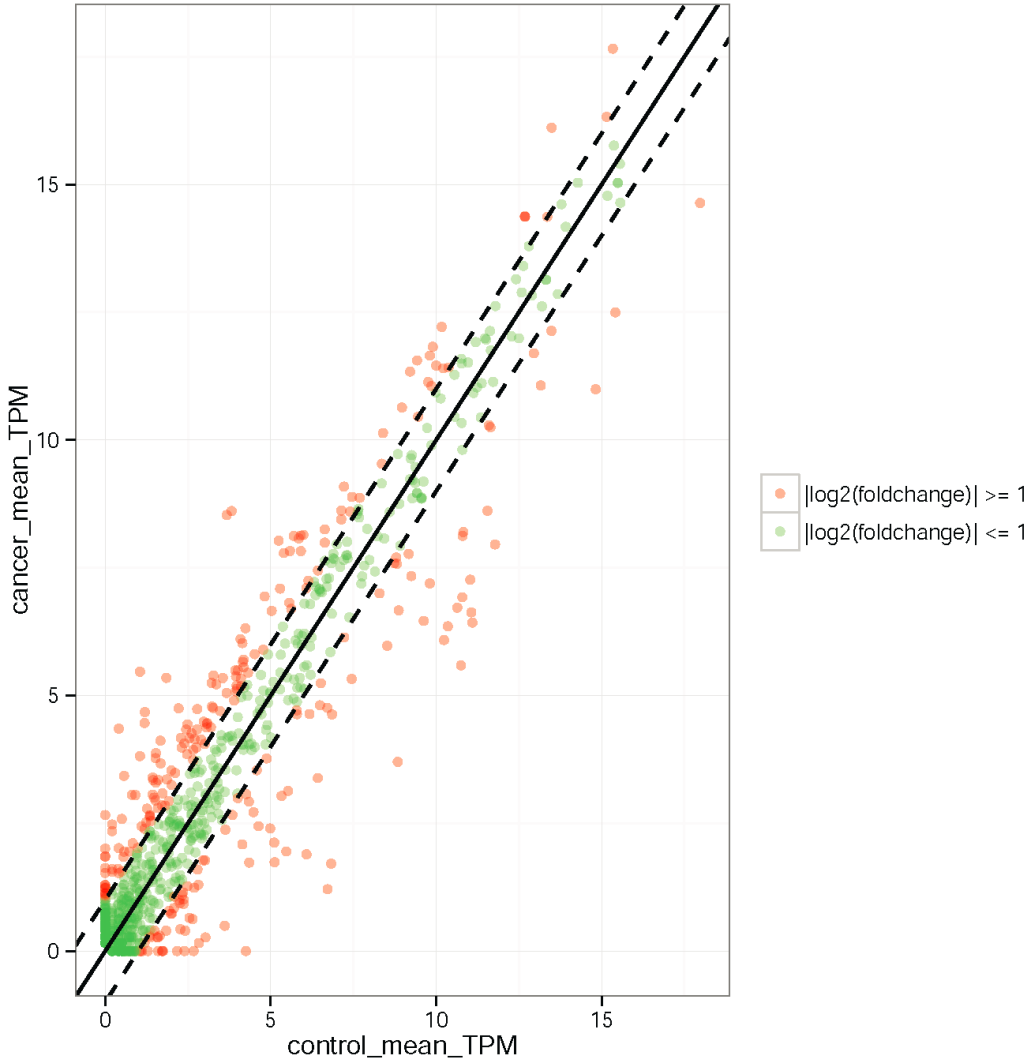


**Fig. 8 Relative expression of miRNAs in ENA and para-cancerous tissues**. The *x*- and *y*-axes indicate the mean TPM expression levels of the miRNAs in each tissue. The red circles represent miRNAs with a fold change ≥ 2; green circles represent miRNAs with a fold change ≤ 2; the points on the dotted line represent miRNAs with a fold change = 2. Fold changes were calculated as the mean miRNA TPM in ENA/mean miRNA TPM in para-cancerous tissues.

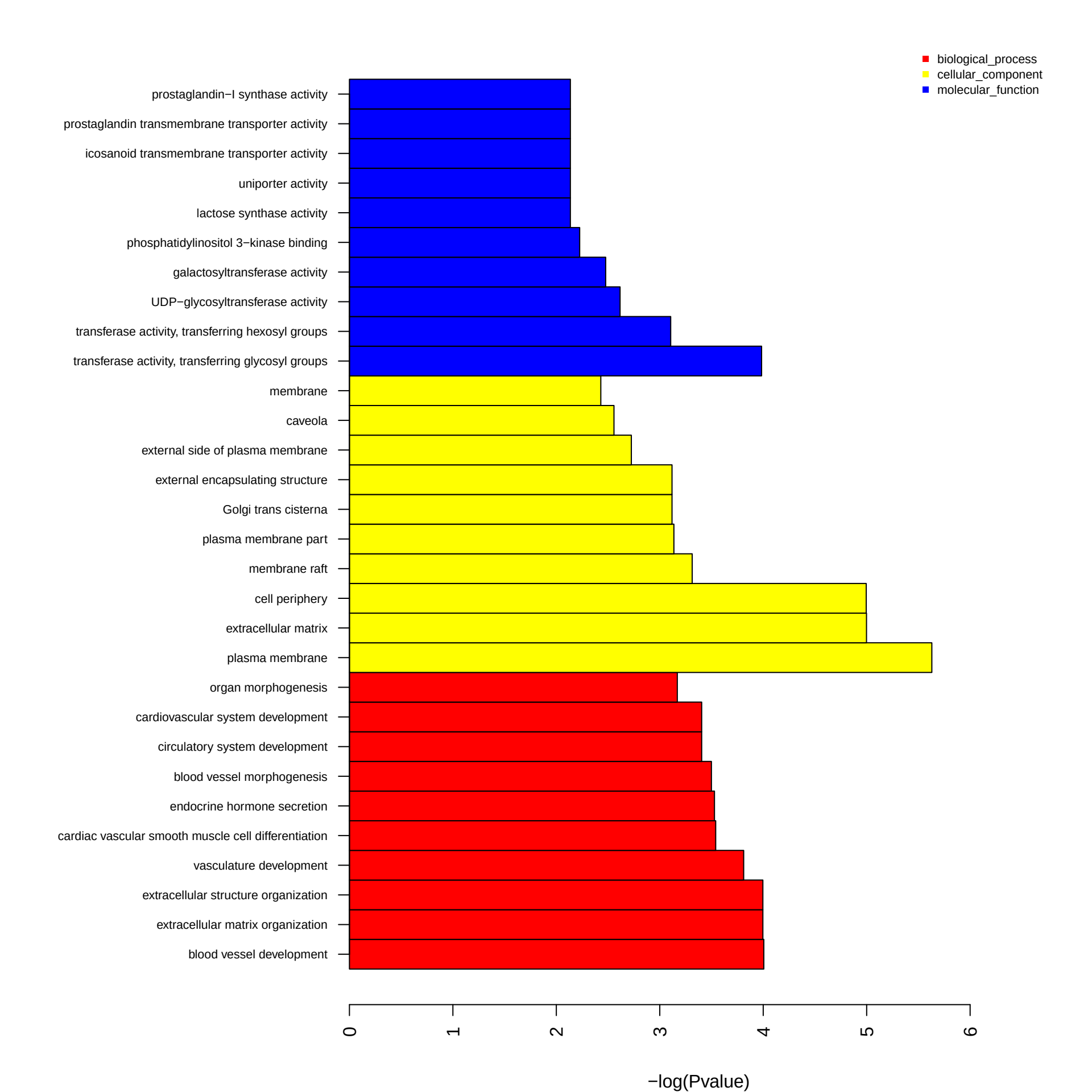
biological_process
cellular_component
molecular_function
prostaglandin−I synthase activity
prostaglandin transmembrane transporter activity
icosanoid transmembrane transporter activity
uniporter activity
lactose synthase activity
phosphatidylinositol 3−kinase binding
galactosyltransferase activity
UDP−glycosyltransferase activity
transferase activity, transferring hexosyl groups
transferase activity, transferring glycosyl groups
membrane
caveola
external side of plasma membrane
external encapsulating structure
Golgi trans cisterna
plasma membrane part
membrane raft
cell periphery
extracellular matrix
plasma membrane
organ morphogenesis
cardiovascular system development
circulatory system development
blood vessel morphogenesis
endocrine hormone secretion
cardiac vascular smooth muscle cell differentiation
vasculature development
extracellular structure organization
extracellular matrix organization
blood vessel development
0
1
2
3
4
5
6
−log(Pvalue)

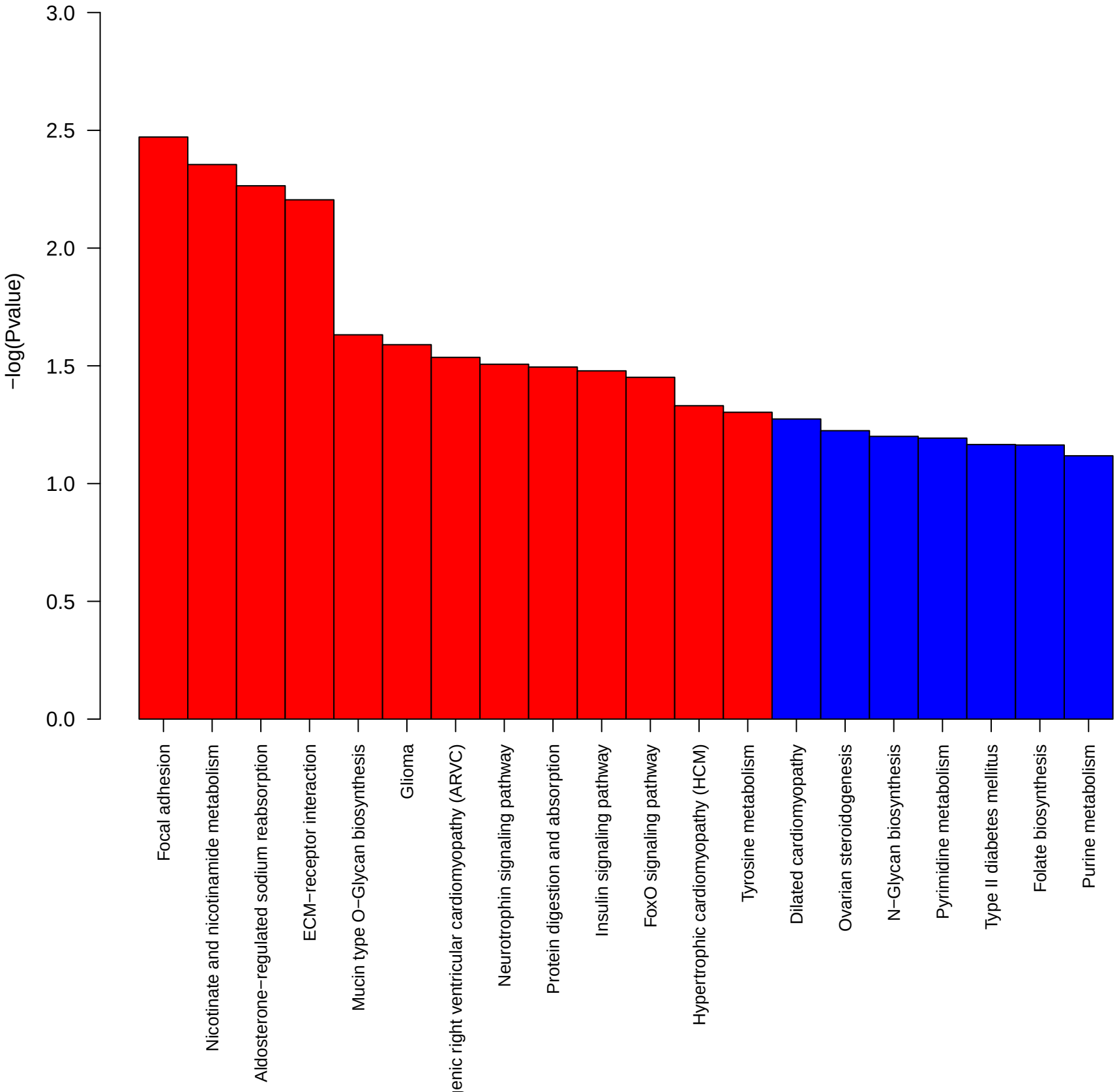
−log(Pvalue)
3.0
2.5
2.0
1.5
1.0
0.5
0.0
Focal adhesion
Nicotinate and nicotinamide metabolism
Aldosterone−regulated sodium reabsorption
ECM−receptor interaction
Mucin type O−Glycan biosynthesis
Glioma
genic right ventricular cardiomyopathy (ARVC)
Neurotrophin signaling pathway
Protein digestion and absorption
Insulin signaling pathway
FoxO signaling pathway
Hypertrophic cardiomyopathy (HCM)
Tyrosine metabolism
Dilated cardiomyopathy
Ovarian steroidogenesis
N−Glycan biosynthesis
Pyrimidine metabolism
Type II diabetes mellitus
Folate biosynthesis
Purine metabolism

**Figure 11** miRNAs expression patterns in nasal tissue

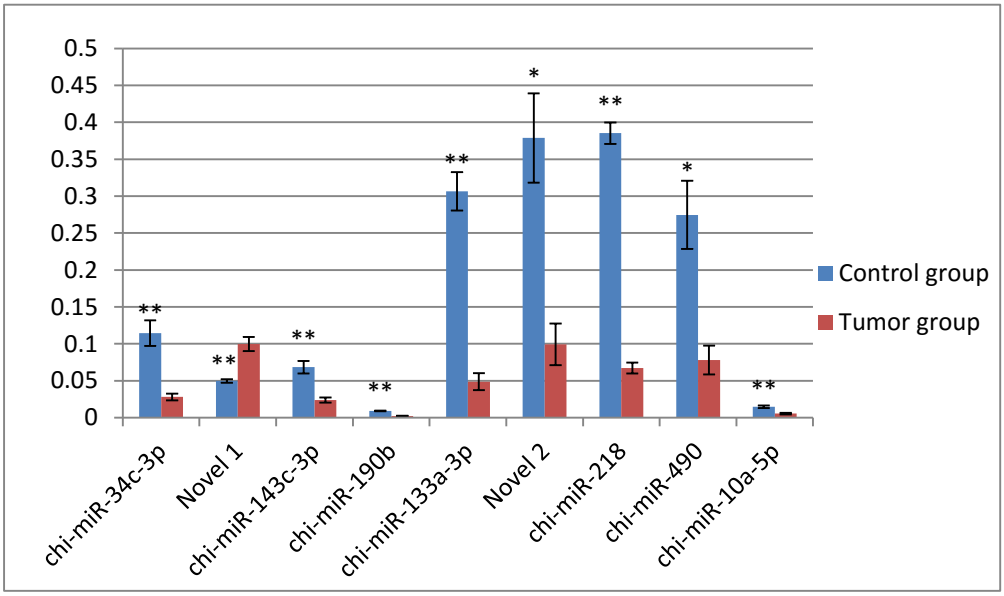


**Fig. 11 qRT-PCR validation of the identified miRNAs using Illumina sequencing technology.** Real-time RT-PCR analysis of nine miRNAs in the tumour and para-carcinoma tissues from 5 goats with ENA. Relative quantification was assessed using the $2^{-\Delta\Delta Cq}$ method and was normalized to *U6* and *GAPDH*. $2^{-\Delta\Delta Ct}$ Means ± SE relative expression levels are presented. * represents $p<0.05$,** represents $p<0.01$.

**Table 1**

**Table 1 The results of clean reads and unique reads maped to the Capra Hircus genome in cancer and control groups.**

| Samples | Clean reads | Total aligned reads | Total aligned reads(%) | Total unaligned reads | Total unaligned reads(%) | Unique reads | Unique aligned reads | Unique aligned reads(%) | Unique unaligned reads | Unique unaligned reads(%) |
|---|---|---|---|---|---|---|---|---|---|---|
| S1 | 8009909 | 7174638 | 89.57 | 835271 | 10.43 | 335710 | 239081 | 71.22 | 96629 | 28.78 |
| S2 | 9883394 | 8614567 | 87.16 | 1268827 | 12.84 | 236291 | 149260 | 63.17 | 87031 | 36.83 |
| S3 | 5129861 | 4573796 | 89.16 | 556065 | 10.84 | 204228 | 127183 | 62.28 | 77045 | 37.72 |
| S4 | 4847129 | 4108137 | 84.75 | 738992 | 15.25 | 203603 | 117200 | 57.56 | 86403 | 42.44 |
| S5 | 5269861 | 4598556 | 87.26 | 671305 | 12.74 | 231658 | 154306 | 66.61 | 77352 | 33.39 |
| S6 | 5627178 | 4846400 | 86.12 | 780778 | 13.88 | 225210 | 143168 | 63.57 | 82042 | 36.43 |